

## Optical Properties and Fermi Surface of Nickel

H. EHRENREICH,\* H. R. PHILIPP, AND D. J. OLECHNA

*General Electric Research Laboratory, Schenectady, New York*

(Received 3 May 1963)

Dielectric constants for Ni obtained from reflectance data at room temperature are reported for photon energies extending to 11 eV. The structure at 0.3 and 1.4 eV and that observed by Krinchik and collaborators at nearly the same energies by the ferromagnetic Kerr effect is reinterpreted in terms of interband transitions probably between  $d$  bands and the Fermi surface. Low-energy interband transitions, which would be expected to occur in many transition metals, cause the reflectance in the infrared to fall off more rapidly than in the noble metals. For photon energies above 4 eV there is a marked resemblance between Ni and Cu. The peak in the energy loss function occurs at nearly the same energy in both materials. As a framework for discussing these results, a model for the band structure and Fermi surface of ferromagnetic Ni is proposed. This model consists of a simple adaptation of band calculations for nonferromagnetic Ni and Cu. The two-band structures, which are assumed to correspond to the energy levels of spin-up and spin-down electrons, respectively, are essentially matched at the bottom of the  $4s$  band. The resulting exchange splitting of the  $d$  band is about 2 eV. A Fermi level appropriate to the required  $s$  and  $d$  electron concentration is postulated. The resulting Fermi surfaces consist of three electron sheets and unimportant hole pockets. One electron surface, corresponding to the spin-down carriers, is copper-like. The remaining surfaces do not contact any zone faces. They are characterized by large anisotropies in electron velocities and large corresponding differences between optical and thermal masses. These results are consistent with the magnetoresistance and Hall effect measurements of Fawcett and Reed and are in semiquantitative agreement with the observed structure in the optical properties, the magneton number, the electronic specific heat, and the plasma frequency.

### 1. INTRODUCTION

IN an earlier paper<sup>1</sup> the optical properties of Cu and Ag were interpreted in terms of intra- and interband single-electron excitations as well as collective plasma effects using rather accurate band calculations<sup>2</sup> as a basis for the discussion. A similar study of Ni appeared of particular interest, since this material is ferromagnetic, while being still very similar to Cu in other respects. Ni has the same crystal structure as Cu, lies next to it in the periodic table, and is miscible in all proportions without any intervening ordered phases. Furthermore, reliable band calculations for its nonferromagnetic state are now becoming available.<sup>3</sup> Even more important, the experimental results for the high-field Hall effect and their interpretation discussed by Fawcett and Reed<sup>4</sup> together with earlier work concerning the magnetoresistance,<sup>5</sup> indicate that an itinerant picture for the ferromagnetic electrons<sup>6</sup> is probably valid. They also impose several important conditions concerning the topology of the Fermi surface in Ni: One surface must be multiply connected as in Cu, while the other surfaces must be such as to yield a high-field Hall coefficient of exactly unity. In the absence of band calculations including realistic treatments of the exchange interaction, the immediate problem is to find a model for the band structure of ferromagnetic Ni, based on existing

calculations and a minimum number of additional assumptions, which leads to Fermi surfaces satisfying these conditions, and is consistent with the optical properties as well as other experimental information. This paper presents such a model in addition to new optical results. The latter are discussed in Sec. 2; the proposed model and Fermi surface are presented in Sec. 3. In Sec. 4, it is shown that the model and Fermi level yield results which are semiquantitatively consistent with the total number of electrons and the magneton number, the optical properties including the ferromagnetic Kerr effect,<sup>7</sup> the magnetoresistance<sup>5</sup> and Hall effect,<sup>4</sup> the electronic specific heat,<sup>8</sup> and the plasma frequency. The free carrier optical region as well as the dc electrical conductivity are also discussed briefly.

### 2. OPTICAL PROPERTIES

The reflectance of electrolytically etched Ni was measured at nearly normal incidence to 11 eV at room temperature using previously described techniques.<sup>1</sup> The results are shown in Fig. 1 together with those for Cu indicated by the dashed curve. For the reasons already mentioned and others to be given in the next section, Cu represents a particularly useful basis for comparison. There is a marked similarity in the optical properties of the two materials above about 4 eV but an appreciable difference at lower energies. The reflectance of Ni falls off rather more rapidly and on the present energy scale does not exhibit the flat, nearly perfectly reflecting region characteristic of Cu and many other metals. A Kramers-Kronig analysis<sup>1</sup> yields the quanti-

\* Present address: Division of Engineering and Applied Physics, Harvard University, Cambridge, Massachusetts.

<sup>1</sup> H. Ehrenreich and H. R. Philipp, *Phys. Rev.* **128**, 1622 (1962).

<sup>2</sup> B. Segall, *Phys. Rev.* **125**, 109 (1962); G. A. Burdick, *ibid.* **129**, 138 (1963).

<sup>3</sup> J. G. Hanus, MIT Solid State and Molecular Theory Group Quarterly Progress Report No. 44, 29, 1962 (unpublished).

<sup>4</sup> E. Fawcett and W. A. Reed, preceding paper, *Phys. Rev.* **131**, 2463 (1963).

<sup>5</sup> E. Fawcett and W. A. Reed, *Phys. Rev. Letters* **9**, 336 (1962).

<sup>6</sup> C. Herring, *J. Appl. Phys.* **531**, 3 (1960) and references cited therein.

<sup>7</sup> G. S. Krinchik and R. D. Nuralieva, *Zh. Eksperim. i Teor. Fiz.* **36**, 1022 (1959) [translation: *Soviet Phys.—JETP* **9**, 724 (1959)]. G. S. Krinchik and A. A. Gorbacher, *Fiz. Metal. i Metalloved.* **11**, 203 (1961).

<sup>8</sup> W. H. Keesom and C. W. Clark, *Physica* **2**, 513 (1935).

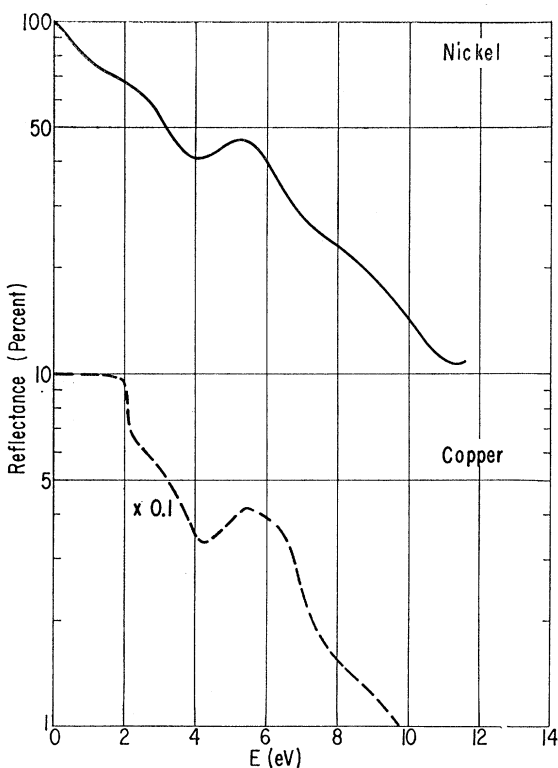


FIG. 1. Spectral dependence of the reflectance of Ni and Cu. The Cu data are those of Ref. 1.

ties plotted in Fig. 2, again compared with the corresponding ones for Cu. Shown are the real and imaginary parts of the frequency-dependent dielectric constant,  $\epsilon_1(\omega)$  and  $\epsilon_2(\omega)$ , a portion of the energy loss function,  $-\text{Im}\epsilon^{-1}(\omega)$ , and the real part of the conductivity,  $\sigma(\omega) = \omega\epsilon_2(\omega)/4\pi$ , whose utility in the present context stems from its less rapid variation at small frequencies. Since  $\epsilon_2(\omega)$  becomes infinite at zero frequency, whereas  $\sigma(\omega)$  remains finite, any structure in the optical constants at low frequencies will be much more evident in the conductivity. Examination of this function reveals that the previously identified<sup>1</sup> interband transition in Cu near 2 eV has disappeared, and in its place in Ni, one finds two pieces of structure at about 0.3 and 1.4 eV. This structure has been observed previously by Beatty and Conn<sup>9</sup> and Roberts<sup>10</sup> in measurements that determined both optical constants  $n$  and  $k$  directly in a range extending from about 0.1 to 3.4 eV. The present experimental results are in excellent agreement over this range.

Roberts<sup>10</sup> fit his results to an analytical expression adapted from a formula due to Drude which contains both free electron and oscillator-like terms. The structure at 0.3 eV was explained by invoking several types of free carriers. One high-mobility carrier was assigned to account for the magnitude of the dc conductivity, and

two other extremely low-mobility carriers characterized by relaxation times  $\tau$  of order  $10^{-16}$  sec were parameterized to dominate above 0.3 eV and produce the observed change of slope. The structure at 1.4 eV, on the other hand, was fitted by an oscillator-like term, and, thus, in more conventional language, associated with an interband transition.

In the present paper, we shall present arguments showing why it is likely that *both* shoulders in  $\sigma$  are associated with interband effects involving transitions for each of the two spin distributions between the  $d$ -band and the Fermi surface. As will be seen, this interpretation leads to an estimate of the ferromagnetic splitting of the  $d$  band in the region of the Brillouin zone surrounding  $L$ .

There are several arguments tending to support the identification of the 0.3-eV structure in terms of interband transitions. The most convincing is based on experimental results for the ferromagnetic Kerr effect by Krinchik and collaborators.<sup>7</sup> They have observed well-defined resonance structure near both 0.3 and 1.4 eV. The 1.4-eV structure was interpreted in terms of transitions between  $3d$  and  $4s$  bands; that at lower energy was associated with the reorientation energy of the electron spin magnetic moment in the exchange field of a ferromagnet. While we wish to propose a different explanation of the low-energy structure, we regard its oscillator-like character as a demonstration that it is unlikely to be associated with free carrier effects.

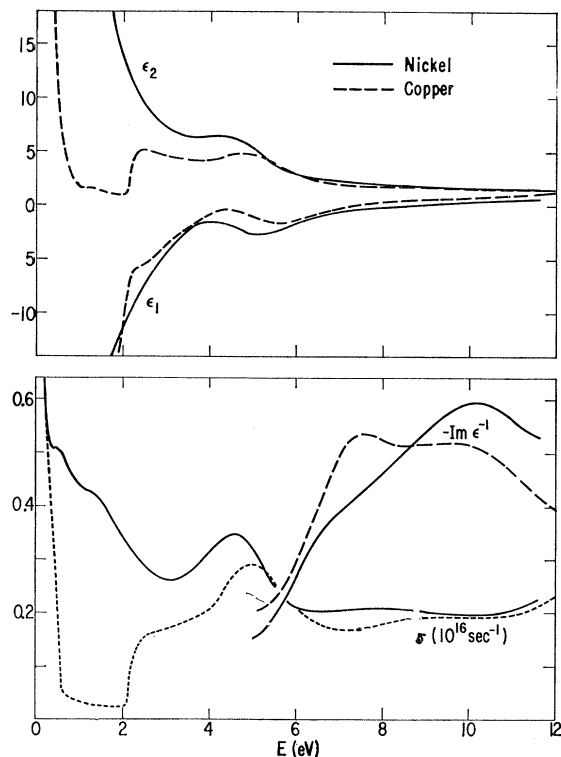
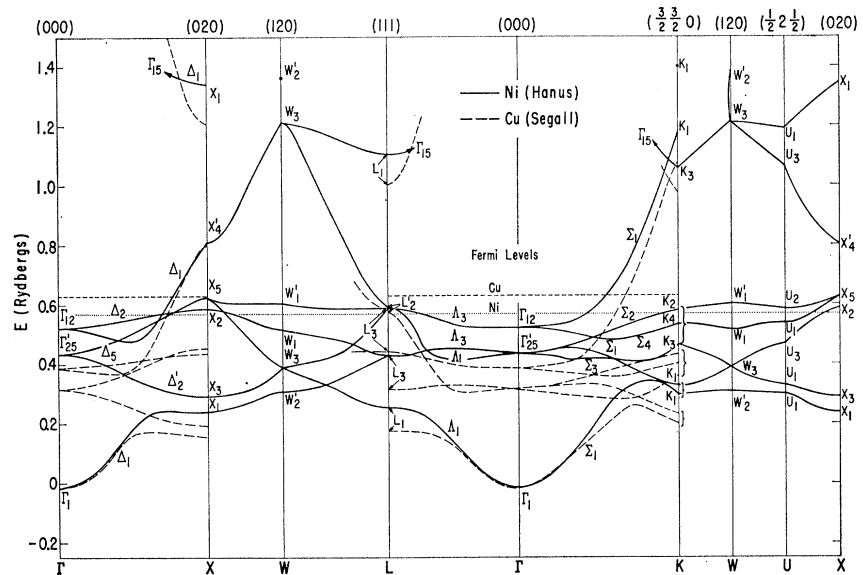


FIG. 2. Spectral dependence of real and imaginary parts of dielectric constant, real part of conductivity, and energy loss function  $-\text{Im}\epsilon^{-1}$  for Ni and Cu.

<sup>9</sup> J. R. Beatty and G. K. T. Conn, *Phil. Mag.* **46**, 989 (1955).

<sup>10</sup> S. Roberts, *Phys. Rev.* **114**, 104 (1959).

FIG. 3. Calculated energy bands of Ni (solid curves) and Cu (dashed curves) according to Hanus (Ref. 3) and Segall (Ref. 2). Cu Fermi level is taken from Segall's calculations. Ni Fermi level is appropriate to band structure model for ferromagnetic state in which solid and dashed curves are associated, respectively, with  $\uparrow$  and  $\downarrow$  electrons.



The remaining arguments are more circumstantial. The first concerns the fact that Roberts' data<sup>10</sup> shows the dielectric constants above 0.3 eV to be nearly temperature-independent, in contrast to those of Cu. One would expect free carrier effects to exhibit an appreciable temperature dependence, especially in Ni in view of the results reported in Ref. 4. If Roberts' assertion,<sup>10</sup> that at room temperature there exist very low mobility carriers, and if Fawcett and Reed's statement,<sup>4</sup> that at 4°K all carriers are in the high magnetic field range above 20 kOe, are to be both correct, it is necessary to invoke a conductivity for the low-mobility carriers which is a very rapidly varying function of temperature. In particular, one would expect the behavior of  $\sigma$  around 0.3 eV to change appreciably with decreasing temperature as the low-mobility carriers become more and more mobile. There is no evidence for such behavior in the experimental data of Refs. 9 and 10. Unfortunately, some ambiguities remain in this argument; the linearity of the Hall coefficient with magnetic field reported in Ref. 4 implies only that there are no carriers having relaxation times that are less than one hundred times smaller than the most mobile ones. Carriers characterized by mobilities appreciably smaller than that would be undetected. The relaxation times for Roberts' slow carriers together with their larger mass are such as to place them in the "undetectable" range, if their temperature dependence is no faster than that of the mobile carriers. Thus, the possibility *both* of an interband transition at 0.3 eV *and* the presence of very sluggish free carriers cannot be completely excluded by the experimental evidence.

The remaining argument deals with the fact, to be discussed in the next section, that band calculations for Ni predict the presence of interband transitions in this range of energies. This is a consequence of the intersec-

tion of the *d*-band complex with the Fermi level. Indeed, the gradual drop of the reflectance in this range, which results from these low-energy transitions, appears to be characteristic of most metals like Fe, Co, and Pd in which the *d* bands play a prominent role.<sup>11</sup>

To complete the discussion of Fig. 2, we note that all the plotted quantities for Cu and Ni show a marked resemblance above about 4 eV, just as the reflectance. Of particular interest is the strong peak of the energy loss function  $-\text{Im}\epsilon^{-1}$  at 10 eV. The behavior of  $\epsilon_1$  and  $\epsilon_2$  in this range indicates that this peak, as the corresponding peak in Cu,<sup>1</sup> is associated with a plasma resonance. These results are in reasonable agreement with the plasma peak at 8.3 eV found from characteristic energy loss experiments.<sup>12</sup> It is interesting that the plasma frequencies of Cu and Ni appear to be in such close correspondence, whereas the electronic specific heats<sup>8,13</sup> differ by an order of magnitude. Clearly, a valid model for the band structure and Fermi surface must be able to explain the reason for this difference.

### 3. BAND STRUCTURE AND FERMI SURFACE

Hanus<sup>3</sup> has recently reported band calculations for nonferromagnetic Ni which interpolate very well between results of corresponding calculations for Cu<sup>2</sup> and face-centered cubic iron.<sup>14</sup> The solid curves in Fig. 3 represent Hanus's results along various directions in and on the surface of the Brillouin zone appropriate to the fcc lattice. The dashed curves represent Segall's<sup>2</sup> re-

<sup>11</sup> Landoldt-Börnstein, *Zahlenwerte und Funktionen* (Springer Verlag, Berlin, 1962) 8. Teil: Optische Konstanten, p. 18.

<sup>12</sup> J. L. Robins and J. B. Swan, Proc. Phys. Soc. (London) **76**, 857 (1960).

<sup>13</sup> Landoldt-Börnstein, *Zahlenwerte und Funktionen* (Springer Verlag, Berlin, 1961) 4 Teil: Kalorische Zustandsgrößen, p. 474.

<sup>14</sup> J. H. Wood, MIT Solid State and Molecular Theory Group Quarterly Progress Report No. 33, 22, 1959 (unpublished).

sults for Cu along principal directions, matched to the Ni calculations at  $\Gamma_1$ , the bottom of the conduction band. The  $d$ -band complex is seen to move more or less rigidly to higher energies as one proceeds from Cu to Ni. In addition, the  $d$  bands broaden. As a guide to the accuracy of these calculations, it should be noted that Burdick's results for Cu,<sup>2</sup> obtained from the same augmented plane wave (APW) technique as Hanus's,<sup>3</sup> are in very good agreement with Segall's calculations<sup>2</sup> which utilized the Green's-function method. Both predict the correct Fermi surface and separation between the Fermi level and  $d$  band. The calculated Fermi level for Cu is that shown by the dashed line in Fig. 3. The dotted line is associated with the model for *ferromagnetic* Ni to be discussed below, and is not appropriate for Hanus's band structure without modification. The relative position of  $s$  and  $d$  bands depends very sensitively on the chosen crystal potential and is, therefore, rather difficult to determine accurately. In comparing the reliability of the Cu and Ni calculations, it is probably only this parameter in Ni that may be less certain.<sup>15</sup>

The exchange interaction, which gives rise to ferromagnetism, will split the  $d$  and  $s$  bands corresponding to the two spin distributions. Callaway's band calculation for<sup>16</sup> ferromagnetic bcc Fe indicates that the splitting of the  $s$  bands may be rather smaller than that of the  $d$  bands. It should be emphasized, however, that the origin of the exchange forces which align the spins is still a controversial subject, and, in any case, may differ appreciably from material to material. Herring's review paper<sup>6</sup> summarizes very clearly the various divergent viewpoints. Any attempt at a reliable *a priori* estimate of exchange splittings is, therefore, premature.

As a temporary substitute, we should like to propose an approximate *model* for Ni, which relies heavily on already existing band calculations but whose limited number of assumptions must be regarded as tentative until they can be justified by fundamental theoretical arguments. At present, this proposal should be judged by its success in describing a variety of experimental information and its usefulness in providing an explicit frame of reference for interpretative purposes.

We shall assume that the particular superposition of the nonferromagnetic Ni and Cu band structures, shown in Fig. 3, is actually a good representation of the band structure of ferromagnetic Ni. This means that after matching the Cu and Ni results at  $\Gamma_1$ , we shall regard the Cu curves to correspond to one spin distribution ( $\downarrow$ ), and the Ni curves to correspond to the other ( $\uparrow$ ). Further, we shall suppose that the Fermi level at 0.57 Ry indicated by the dotted line in Fig. 3 is characteristic of the ferromagnetic Ni band structure. It should be noted, however, that as long as the lower  $d$  band is completely filled and the bands are assumed rigid with

respect to changes in the splitting, the position of the Fermi level will be *independent* of the splitting.

It should be emphasized that the band structure for each spin is calculable from a given crystal potential. With one very minor exception, there has been no arbitrary adjustment of band gaps or curvatures for electrons of a given spin which would not be derivable from such a potential. Our basic assumption may thus be stated as follows: The exchange potential giving rise to the ferromagnetic splitting is taken to be equal to the difference between potentials for the Cu and Ni crystals plus a constant which aligns the  $\Gamma_1$  levels of the two spins. Since one expects the ferromagnetic interaction to split the two sets of  $d$  bands symmetrically, one moving up as far as the other moves down, the  $d$  bands of nonferromagnetic Ni, according to the present model, would be lowered with respect to  $\Gamma_1$  by about 0.8 eV from those calculated by Hanus.<sup>3</sup> A shift of this magnitude still permits the Ni results to interpolate well between those already mentioned for fcc Fe and Cu.

The present model was suggested by existing experimental evidence, most notably the magnetoresistance experiments of Fawcett and Reed<sup>5</sup> which showed one of the Fermi surfaces of Ni to be copper-like, and the optical experiments discussed in the preceding section which can be interpreted consistently, but not uniquely, within this framework. Its experimental consequences are discussed in detail in the following section.

The small arbitrary adjustment of the band structure, referred to above, consists of lowering the  $L_2'$  level for the  $\downarrow$  copper-like electrons by about 0.02 Ry. As we shall see, this change produces the experimentally observed area of contact with the (111) faces of the Brillouin zone, without affecting other properties appreciably.

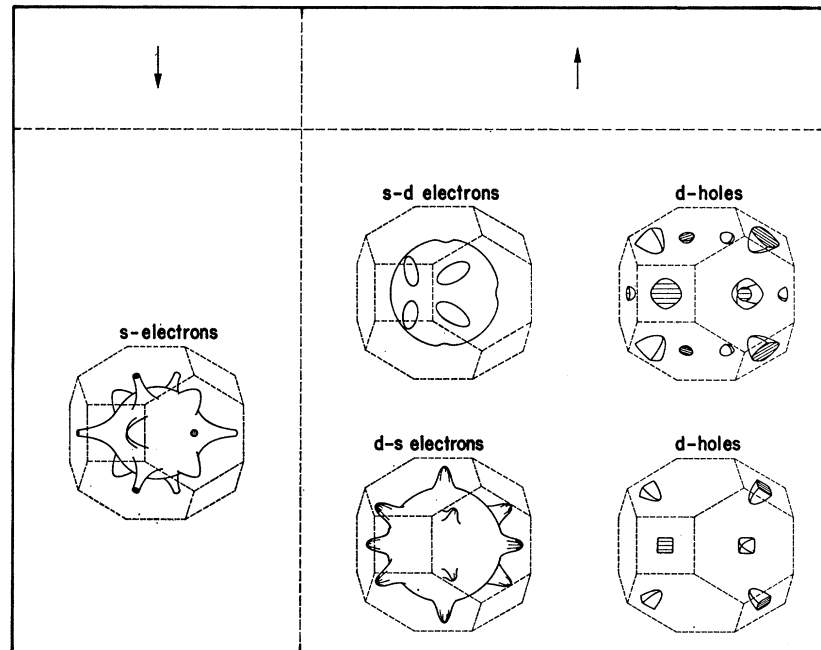
The Fermi surfaces corresponding to the two spins,  $\uparrow$  and  $\downarrow$ , which result from the band structure and Fermi level of Fig. 3, are shown in Fig. 4. In constructing the surfaces for the  $\uparrow$  electrons, for which the Fermi level intersects a number of different  $E$  versus  $k$  curves, it should be remembered that the energy values corresponding to a given sheet of Fermi surface must be determined such that to every  $k$  the values belong to the same member of the sequence arranged in order of increasing energies. In particular, it is necessary to keep track of degeneracies in the labeling, and to pass from one branch of  $E(k)$  to another at points of accidental degeneracy.

The Fermi surface corresponding to the  $\downarrow$  electrons (dashed curves in Fig. 3) is topologically the same as Cu. Because the Fermi level lies below that of Cu, the neck diameter is reduced and other portions of the surface are somewhat contracted towards  $\Gamma$ . The [110] directions are pulled in more than the [100] directions with the effect that the bulges along [100] are accentuated with respect to those in copper. The lowering of the Fermi level, of course, also reduces the density of electrons contained within the surface. The  $\downarrow$   $d$  bands are

<sup>15</sup> We are grateful to Professor J. C. Slater for a comment concerning this point.

<sup>16</sup> J. Callaway, Phys. Rev. **99**, 500 (1955)

FIG. 4. Fermi surfaces of ferromagnetic Ni for spin  $\uparrow$  and  $\downarrow$  carriers.



completely filled and do not contribute to the Fermi surface.

This is not the case for the  $\uparrow$  electrons and the situation is correspondingly more complicated. In discussing the properties of the surfaces shown in Fig. 4 along various directions, it will be necessary to distinguish whether the electrons moving along these directions are "s-like" or "d-like." These terms will be taken to be descriptive of the electron velocities, that is, the slopes  $\nabla_{\mathbf{k}}E$  rather than the symmetry of the wave functions. The somewhat broad, roughly parabolic  $s$  bands threading their way through the much flatter and narrower  $d$  bands are qualitatively quite apparent in Fig. 3. For most portions of the  $E$  versus  $\mathbf{k}$  curves intersecting the Fermi level, the assignment  $s$ - or  $d$ -like in this sense can be made quite unambiguously. For example, the  $\Delta_1$  intersection is  $s$ -like, where  $\Delta_2$  is  $d$ -like.

The Fermi surfaces of the  $\uparrow$  electrons consist of two electron surfaces and two sets of hole pockets. Both electron surfaces are basically spherical, but one has dimples and the other has bulges along (110) directions. Neither surface contacts any zone face. The remarkable feature is that they are  $s$ -like or  $d$ -like in the above sense along different directions in  $\mathbf{k}$  space. Thus, the dimpled surface, containing what we shall call  $s$ - $d$  electrons, is  $s$ -like in  $[110]$ , but  $d$ -like along other principal directions. The bulged surface, to be denoted  $d$ - $s$ , is  $s$ -like along  $[100]$ , but  $d$ -like in other principal directions. The hole pockets are  $d$ -like and are centered on (111) and (100) faces for one set and (111) faces for the other. They will be seen to contribute little to the physical properties under discussion here.

It should be emphasized that the region of  $\mathbf{k}$  space de-

scribed by the band structure in Fig. 3 is somewhat too small to permit accurate estimates of the extent of the bulges, dimples, and necks. Thus, even if we assume that the proposed model is *precisely* correct, the calculations of volumes and particularly surface areas of the geometrical shapes shown in Fig. 4 cannot be regarded as accurate to better than 20-30%. In this connection, however, it is worth reiterating again that the results used to sketch the Fermi surfaces for the  $\downarrow$  and  $\uparrow$  electrons are characteristic of actual band calculations for Cu and Ni, respectively, and a Fermi level which will be seen to yield very closely the required number of electrons per atom.

The number of electrons per atom is calculated very simply from the volume of the occupied region of the Brillouin zone, remembering that in the presence of the ferromagnetic splitting each zone is able to accommodate one electron per atom. Fawcett and Reed<sup>4</sup> have emphasized this fact by renaming the zones in ferromagnetic materials "spin zones." The results for each surface are shown in Table I. The hole pockets are seen to make only a small contribution.

The  $s$  and  $d$  character along different directions for

TABLE I. Parameters for ferromagnetic Ni deduced from Fig. 3.

	$s$ electrons	$s$ - $d$ electrons	$d$ - $s$ electrons	holes
Electrons/atom	0.33	0.21	0.39	0.04
Thermal mass, $m_t/m$	1.7	8.0	7.1	
Optical mass, $m_o/m$	1.4	3.4	3.5	
$\langle v \rangle_F$ ( $10^7$ cm/sec)	10	2.7	3.9	
$\langle v^{-1} \rangle_F$ ( $10^{-8}$ sec/cm)	1.2	4.9	4.3	
$S_F/S_F^o$	1.03	1.3	1.1	

the  $s$ - $d$  and  $d$ - $s$  electrons results in rather large anisotropies in the electron velocities. Some values along principal directions are shown in Table I. This anisotropy has a profound effect on values of the thermal and optical masses,  $m_t$  and  $m_o$ , respectively. These masses, for each type of carrier, may be expressed in the form<sup>17</sup>

$$\begin{aligned} m_t &= \hbar k_F (S_F/S_F^0) \langle v^{-1} \rangle_F, \\ m_o &= \hbar k_F (S_F^0/S_F) \langle v \rangle_F^{-1}, \end{aligned} \quad (1)$$

where  $\langle v \rangle_F = S_F^{-1} \int v dS_F$  represents the velocity averaged over the Fermi surface  $S_F$ , and  $S_F^0$  is the surface area of the equivalent sphere, having radius  $k_F$ , containing the same electron density as the actual Fermi surface. The magnitude of  $\langle v^{-1} \rangle_F$  is determined by the slow velocity  $d$ -like directions, whereas that of  $\langle v \rangle_F$  is dominated by the fast  $s$ -like directions. The anisotropic velocities cause  $\langle v^{-1} \rangle_F$  and  $\langle v \rangle_F^{-1}$  to be considerably different, or, in terms of Schwarz's inequality,  $\langle v \rangle_F \langle v^{-1} \rangle_F$  to be rather larger than unity. The optical and thermal masses, according to Eq. (1), will then also differ appreciably. This difference is enhanced further by the factor  $(S_F/S_F^0)^2$  which is involved in  $m_t/m_o$ . Because of the relatively large distortion of the actual Fermi surface, its area  $S_F$  is somewhat larger than that of the equivalent sphere  $S_F^0$ .

The velocity averages were computed using the band structure results along [100], [110], and [111] directions and established numerical procedures.<sup>18</sup> For reasons to be discussed in the following section, the necks corresponding to the  $s$  electrons were replaced by cylinders having  $\frac{1}{4}$  the diameter of those for Cu and the same neck mass. Values for the parameter just discussed are given in Table I. Since the band calculations of Fig. 3 do not specify very precisely the extent of the distortions, and the surface areas are particularly sensitive to them, the values of  $S_F$  are somewhat uncertain, but again, by probably no more than 30%.

The resulting thermal and optical masses are also shown in Table I. Two qualitative features are to be noted in particular. First, some of the masses are extraordinarily large. This stems from the fact that some portions of the  $d$  band, such as, for example,  $\Delta_2$  which determines the velocity of the  $s$ - $d$  electrons along [100] directions, are extremely narrow. Second, the thermal and optical masses for the  $\uparrow$  electrons differ quite appreciably.

#### 4. RESULTS AND DISCUSSION

The various subsections which follow deal with the interpretation of optical and other experimental data in terms of the band structure and Fermi surface just discussed. In the variety of cases considered here, we obtain semiquantitative agreement between experimental data and the corresponding theoretical results

<sup>17</sup> M. H. Cohen, *Phil. Mag.* **3**, 762 (1958).

<sup>18</sup> D. D. Betts, A. B. Bhatia, and M. Wyman, *Phys. Rev.* **104**, 37 (1956).

deduced from our model. This holds particularly for the topological results of Fawcett and Reed<sup>4,5</sup> concerning the Fermi surface. The itinerant description of the electrons in Ni, therefore, appears to be valid. On the other hand, at the present time, the tentative identification of optical structure in terms of interband transitions in given regions of the Brillouin zone must be viewed with considerable caution.

#### A. Electron Concentration and Magnetron Number

According to the results in Table I, the number of  $\downarrow$  and  $\uparrow$  electrons in  $3d$  and  $4s$  shells is 5.3 and 4.6 per atom, respectively. Thus, the total electron concentration is 9.9 in comparison to the expected 10 per atom. The magnetron number is 0.7, in comparison to the experimentally observed value of 0.6. The extent of agreement indicates that the Fermi level has been fixed at nearly the correct energy with respect to the band structure in Fig. 3. As already pointed out, its position, according to the present model, is independent of the assumed splitting as long as the lower  $d$  band is completely filled.

#### B. Magnetoresistance and Hall Effect

The aspects of the experimental results<sup>4,5</sup> which are of particular interest here are the following: (1) Magnetoresistance measurements indicate that at least one of the electron surfaces is copper-like with neck radius roughly  $\frac{1}{4}$  that of Cu; (2) the high-field Hall coefficient at helium temperature corresponds very closely to that appropriate to 1 electron per atom and shows from its dependence on magnetic field that all carriers are likely to be in the high-field range.

The Fermi surface for the  $\downarrow$  electrons in Fig. 4 is, indeed, copper-like. Figure 5 shows a detail of the band structure of Fig. 3 in the vicinity of  $L$  with the minor adjustment of the  $L_{2'}$  level already discussed. It is seen that according to the present model the reduced neck radius in Ni results from the lowering of the Fermi level. The model implies that the neck mass of Ni should be

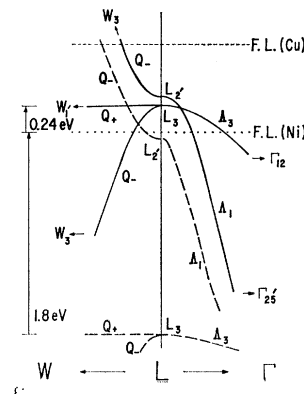


FIG. 5. Detail of the band structure shown in Fig. 3 in the vicinity of  $L$ .

about the same as that in Cu. Cyclotron resonance experiments<sup>19</sup> would be useful in settling this point.

The Fermi surfaces of Fig. 4 are also consistent with the observed Hall coefficient and Fawcett and Reed's<sup>4</sup> explanation of how this can come about. To paraphrase their argument simply for the special case of Ni we might say the following: There are 12 energy sheets corresponding to the  $3d$  and  $4s$  electrons which are occupied by 10 electrons. Seven of them are completely filled. Three contain electrons and the remaining two contain holes. If  $n_i$  and  $h_i$  correspond, respectively, to the number of electrons and holes per atom in a partly occupied sheet, then  $7+n_1+n_2+n_3+(1-h_1)+(1-h_2)=10$ . Thus,  $n_1+n_2+n_3-h_1-h_2=1$ . The left-hand side of the preceding equation is just the quantity determined by the high field Hall coefficient. The fact that this combination corresponds to the observed Hall coefficient indicates that the present Fermi surfaces are consistent with these experiments. The implication that at  $4^\circ\text{K}$  all carriers are sufficiently mobile to be in the high magnetic-field limit supports our earlier statement that the structure in the optical properties discussed by Roberts<sup>10</sup> at 0.3 eV cannot be caused primarily by low-mobility free carriers because of its very weak temperature dependence.

### C. Interband Optical Properties

The optical structure at 0.3 and 1.4 eV discussed in connection with Fig. 2 has been assigned to interband effects. Its presence can be understood in terms of Fig. 5. The 1.4-eV structure may be associated with a transition involving the  $\downarrow$  electrons (dashed curves) between  $Q_+$  and  $Q_-$  at the Fermi level. As indicated on the side of Fig. 5, our model predicts a gap of 1.8 eV, in reasonable agreement with the observed value. This assignment is analogous to that for the 2.2-eV transition in Cu. The low-energy transition at 0.3 eV may be associated with a gap involving the  $\uparrow$  electrons (solid curves) between  $Q_-$  at the Fermi level and  $Q_+$  and  $\Lambda_1$  and  $\Lambda_3$ . As shown in Fig. 5, the corresponding theoretical gap is 0.24 eV.

These interband transitions are the lowest energy vertical excitations along symmetry lines in the Brillouin zone which are permitted by the present band structure model. Optical experiments on Cu-Ni alloys, unfortunately, may not be useful in confirming these assignments because of the possible existence of localized states<sup>20</sup> which would tend to preclude a smooth shift of a given piece of structure as one proceeds from Cu to Ni. We hope to return to this question in a future publication.

This assignment of the 0.3 and 1.4 eV transitions implies that  $L_3$  points of the  $d$  bands corresponding to the two spins are split by about 1.7 eV. According to the

present model, this exchange splitting is roughly the same at other symmetry points. Its magnitude is somewhat greater than the value 0.6 eV deduced by Slater<sup>21</sup> from atomic spectra. Anderson,<sup>20</sup> however, has pointed to the neglect of the exchange self-energy in Slater's treatment which causes his value to be too small. Indeed, the magnitudes given by Anderson<sup>20</sup> are also rather larger than the present result. (*Note added in proof.* Kanamori has recently shown that electron correlation effects provide a substantial reduction of these magnitudes. We are grateful to Professor Kanamori for a preprint of his paper.) An experimental determination of some of the mass parameters determining the Fermi surface for the  $s$  electrons should yield more precise information concerning the location of the deeper  $d$  bands, since they are influenced importantly by these bands.

The identification of the observed optical structure at higher energies is an even more speculative matter. As pointed out in Ref. 1, one expects such structure to be associated with critical points in the joint density of states which are most likely to occur at symmetry points in the Brillouin zone. This viewpoint has been very successful in the interpretation of optical data in semiconductors.<sup>22,23</sup> It has, however, become clear, particularly from Ref. 23, that very extensive calculations are required to demonstrate the location of all important critical points. Indeed, the usefulness of this viewpoint for metals may be limited since the optical structure is much broader, possibly due to convolutions of structure arising from several different transitions or perhaps because of shorter excited state lifetimes brought about by electrons in partly filled bands. Lacking calculations determining the location of critical points, we shall adopt the same viewpoint as that previously used to discuss optical structure in Ag and Cu for the same energy range.<sup>1</sup> Figure 6 shows the absorption coefficient for both Ni and Cu.<sup>1</sup> The arrows in the figure correspond to some of the indicated vertical band gaps predicted by Segall's calculations for Cu and the present model for Ni. One is likely to find critical points at or near these points in  $\mathbf{k}$  space and, therefore, structure in the absorption coefficient. In Ni, of course, there are two different sets of transitions corresponding to each of the two spin distributions as indicated by the large arrows on the right of the figure. The  $\downarrow$  transitions not involving the Fermi surface are the same as in Cu by the definition of our model. The  $\uparrow$  transitions differ somewhat energetically. Indeed, some of them, such as  $X_5 \rightarrow X_4$ , are not present because of the lowering of the Fermi level which leaves the  $X_5$  state unoccupied. There are several pos-

<sup>21</sup> J. C. Slater, Phys. Rev. **49**, 537 (1936).

<sup>19</sup> For example, A. F. Kip, D. N. Langenberg, and T. W. Moore, Phys. Rev. **124**, 353 (1961).

<sup>20</sup> P. W. Anderson, Phys. Rev. **124**, 41 (1961) and cited references.

<sup>22</sup> H. Ehrenreich, H. R. Philipp, and J. C. Phillips, Phys. Rev. Letters **8**, 59 (1962); D. T. F. Marple and H. Ehrenreich, *ibid.* **8**, 87 (1962).

<sup>23</sup> D. Brust, J. C. Phillips, and F. Bassani, Phys. Rev. Letters **9**, 34 (1962).

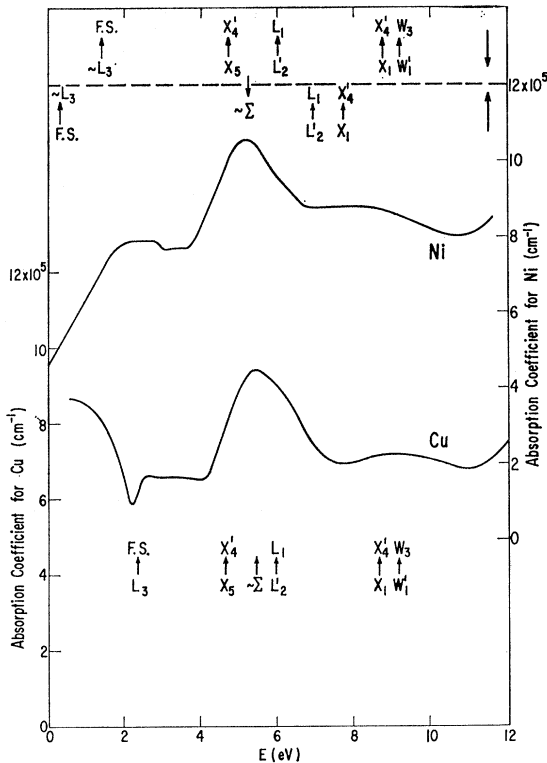


FIG. 6. Spectral dependence of the absorption coefficient for Ni and Cu. The arrows correspond to energies of some of the allowed interband transitions at symmetry points obtained from Fig. 3 for  $\uparrow$  and  $\downarrow$  electrons in Ni, and from Segall's calculations (Ref. 2) for Cu.

sible vertical transitions along  $\Sigma$  whose presence we have just indicated schematically.

The figure shows fairly clearly that these transitions, which correspond to those of lowest energy at symmetry points, indeed coincide with structure in the absorption coefficient. Further, it indicates the possible reason for the similarity in structure in the optical properties of Cu and Ni above 4 eV: Some of the band gaps which may be most important appear to have nearly the same values in both materials. For the reasons already mentioned, it is, however, quite premature to regard the assignments implicitly made in Fig. 6 as anything but suggestive. One discrepancy to be noted, for example, is the fact that the strong, but broad peak near 6 eV is characterized by practically the same absorption coefficient in both Ni and Cu, whereas according to our model one would expect the peak for Ni to be somewhat smaller, unless it is determined entirely by transitions at or near  $\Sigma$ .

#### D. Free Carrier Effects

Because of the onset of interband transitions at such low energies in Ni, it is almost impossible to achieve a separation of the intra and interband contributions of the dielectric constants of the sort that was carried out

in Ag and Cu.<sup>1</sup> It is, however, possible to make some generalized statements concerning the applicability of the Drude formula for the conductivity of free carriers over the energy range 0 to 0.3 eV. For several types of free carriers  $i$ , the formula for the complex frequency dependent conductivity  $\sigma$  may be written in the form

$$\sigma(\omega) = (4\pi)^{-1} \sum_i \omega_{P_i}^2 \tau_i (1 + \omega^2 \tau_i^2)^{-1}, \quad (2)$$

where  $\omega_{P_i}^2 = 4\pi n_i e^2 / m_{ai}$  is the square of the plasma frequency corresponding to the carriers  $i$ ,  $n_i$  is the carrier concentration per unit volume, and  $\tau_i$  is the relaxation time.

We suggest that Eq. (2) is inapplicable to Ni if interband transitions indeed dominate the optical properties above 0.3 eV and if all  $\tau_i$  are constant or a decreasing function of frequency. To support this assertion, it will be necessary to consider averages of the following form:

$$\langle f \rangle = \omega_P^{-2} \sum_i \omega_{P_i}^2 f_i. \quad (3)$$

Here, the total plasma frequency  $\omega_P$  is related to the  $\omega_{P_i}$  by the relationship  $\omega_P^2 = \sum_i \omega_{P_i}^2$ . According to Eqs. (2) and (3),

$$\langle \tau \rangle = 4\pi\sigma(0) / \omega_P^2 = 7 \times 10^{-15} \text{ sec}. \quad (4)$$

This average is determined by the low-frequency behavior of  $\sigma$ . The same equations also permit an evaluation in closed form of

$$\langle \omega^2 \tau / (1 + \omega^2 \tau^2) \rangle = 4\pi\sigma(\omega) (\omega / \omega_P)^2. \quad (5)$$

For high frequencies, such that  $\omega\tau \gg 1$ , the left-hand side becomes  $\langle \tau^{-1} \rangle$ . Schwarz's inequality requires that

$$\langle \tau \rangle \langle \tau^{-1} \rangle \geq 1. \quad (6)$$

This condition must be satisfied for Eq. (4) and the asymptotic form of Eq. (5) if the  $\tau_i$  are independent of frequency or decreasing functions of frequency. If we suppose the structure in  $\sigma(\omega)$  at 0.3 eV, shown in Fig. 2, to be associated with interband contributions, then the intraband contribution must tend rapidly to zero in a way that cannot be very much slower than that indicated by the dashed curve for Cu. A fairly conservative graphical estimate shows that the high-frequency behavior is such that  $\langle \tau^{-1} \rangle < 10^{14} \text{ sec}^{-1}$ . However, this would contradict Eq. (6) unless either Eq. (2) for  $\sigma(\omega)$  is inapplicable or  $\tau_i$  increases with frequency for some of the carriers  $i$ . The latter effect, if dominant, may possibly be associated with rapid variation of the density of states as carriers depart increasingly far from the Fermi surface with increasing frequency or perhaps changes in the character of the quasiparticles with frequency. More extensive optical data in the infrared may be very useful in settling these questions.

The present band structure model also permits some qualitative statements concerning the magnitude of the dc conductivity. If it is assumed that at room temperature the  $\uparrow$  carriers have rather lower mobilities than the  $\downarrow$  copper-like electrons because the latter cannot scatter

easily into the high density of states of the unoccupied  $\uparrow d$ -band states, then the conductivity will be dominated by the  $\downarrow$  electrons. Under these circumstances one would expect, according to the present model, that the relaxation time of the  $\downarrow$  carriers is quite similar to that for the corresponding electrons in Cu. The lower conductivity in Ni would then be associated with the fact that there are only 0.3 such carriers per atom compared to one in Cu. This is in satisfactory agreement with the observed conductivity ratio of about  $\frac{1}{4}$  at room temperature.

### E. Specific Heat and Plasma Frequency

The electronic heat capacity for a ferromagnetic metal containing contributions from various spin zones  $i$  is  $\gamma T$ , where

$$\gamma = (\pi^2/3)(8\pi^3\hbar)^{-1}K^2 \sum_i S_{F_i} \langle v^{-1} \rangle_{F_i}. \quad (7)$$

By Eq. (1), the argument in the sum is directly proportional to the thermal masses  $m_{ti}$ . On the other hand, the plasma frequency  $\omega_P$ , as defined in the preceding subsection, depends only on the optical masses  $m_{oi}$ . We have already determined in Table I all the parameters necessary for the numerical evaluation of the formulas. We find  $\gamma = 5.7 \times 10^3$  ergs/cm<sup>3</sup> °K in comparison to the experimental value  $10.3 \times 10^3$  ergs/cm<sup>3</sup> °K, and  $\hbar\omega_P = 7.7$  eV in comparison to the value 10 eV determined from Fig. 2 and 8.3 eV obtained from Ref. 12. The fact that the computed specific heat is about a factor of 2 below the experimental value is not an unusual outcome of such calculations based on band theory concepts.<sup>24</sup> The agreement of the plasma frequencies is rather better, but somewhat deceptive since  $\omega_{P_i}$  goes as  $(n_i/m_i)^{1/2}$  and thus depends but weakly on the parameters calculated in Sec. 3.

The salient qualitative feature to be noted from these results is the reason for the close similarity in the plasma frequencies of Ni and Cu on the one hand contrasted with the order of magnitude difference between specific heats on the other. This situation results principally from the large differences between optical and thermal masses and the fact that the latter are quite large. The similarity in plasma frequencies arises in addition from the fact that there is a free electron concentration of nearly one per atom. Some of the calculated values of  $m_o$ , however, are too large to render the agreement precise. Further, the oscillator strengths of the  $s$  and/or  $d$  bands are only weakly reduced by 10 eV. An  $n_{\text{eff}}$  plot for Ni, such as that given in Fig. 3 of Ref. 1 for Cu, has

only attained a value 1.6/atom out of a maximum of 10/atom corresponding to the total number of electrons in the  $s$  and  $d$  shells. In addition, the oscillator strength itself is very weak around 10 eV. Thus, the plasma frequency should be determined largely by the free electrons and little affected by the presence of interband transitions.

*Note added in proof.* J. C. Phillips has independently advanced a model for the band structure of ferromagnetic Ni based on Hanus's calculations which is quite similar to that described here. In this model the splitting between the  $d$  bands is taken to be between 0.5 and 0.6 eV, rather than the value 2 eV postulated here. The bands are assumed to move rigidly in the presence of the exchange interaction as in the present model. Since the lower  $d$  band is completely filled, the resulting Fermi level will be very close to that reported here. The Fermi surfaces, and the resulting magnitudes of the specific heat, plasma frequency, and conductivity would also be expected to agree. The band structure giving rise to the neck masses at  $L$  and the 0.3-eV optical transition differs in the two models. Phillips states that the sharp structure at 0.3 eV in the ferromagnetic Kerr effect can only be explained if it is associated with van Hove singularities. The argument, however, is based on the assumption, valid in semiconductors, that the effect arises from the formation of Landau levels, whereas it has been shown<sup>25</sup> that in ferromagnetics the effect arises from changes in the wave function due to the spin-orbit interaction. Preliminary estimates by B. Cooper and H. Ehrenreich indicate that the observed structure can be qualitatively explained on the basis of the present model. The neck mass obtained from Phillips' model would be expected to differ appreciably from that assumed here, which is close to that of Cu. Cyclotron resonance experiments may decide this question. Phillips also points out correctly that the 1.4-eV optical structure might arise from transitions between  $W_1$  and  $W_1'$  for the  $\uparrow$  electrons. We are very grateful to Professor Phillips for communicating his results before publication.

### ACKNOWLEDGMENTS

We are grateful to E. Fawcett and W. A. Reed for a number of stimulating conversations and for communicating some results prior to publication. Our thanks also go to H. Brooks, F. S. Ham, and C. Herring for some helpful comments.

<sup>24</sup> W. A. Harrison (private communication).

<sup>25</sup> P. N. Argyres, Phys. Rev. **97**, 334 (1955).